Robust Nodal *d*-Wave Spectrum in Simulations of a Strongly Fluctuating Competing Order in Underdoped Cuprate Superconductors

W. A. Atkinson,[1,*] J. David Bazak,[1] and B. M. Andersen[2]

[1]*Department of Physics and Astronomy, Trent University, Peterborough, Ontario, Canada K9J 7B8*

[2]*Niels Bohr Institute, University of Copenhagen, DK-2100 Copenhagen, Denmark*

(Received 11 June 2012; published 27 December 2012)

We resolve an existing discrepancy between convincing evidence for competing order in underdoped cuprates and spectroscopic data consistent with a homogeneous *d*-wave superconductor in the very same compounds. Specifically, we show that fluctuations of the competing order generate strongly inhomogeneous states whose spectra are almost indistinguishable from the pure *d*-wave superconductor. This is in contrast to the commonly studied case of homogeneously coexisting order, which typically generates a reconstructed Fermi surface with closed Fermi pockets. The signatures of the fluctuating competing order can be found mainly in a splitting of the antinodal band, and, for strong magnetic order, in small induced nodal gaps similar to those found in recent experiments on underdoped $La_{2-x}Sr_xCuO_4$.

DOI: 10.1103/PhysRevLett.109.267004 PACS numbers: 74.81.−g, 74.40.−n, 74.72.Kf

Many recent experiments point to the prominence of competing phases in underdoped cuprate superconductors, and challenge existing theories for the pseudogap phase [1–10]. Evidence has been found for stripe phases in the La_2CuO_4 [11] and $YBa_2Cu_3O_{6+x}$ families [9,12–14], checkerboard and nematic phases in the Bi-based cuprates [15–17], loop-current order in $YBa_2Cu_3O_{6+x}$ [18], and spin glass phases in most of the highly underdoped cuprates [19–23]. All of these phases are expected to have clear spectroscopic signatures which, in many cases, involve a Fermi surface reconstruction; puzzlingly, angle resolved photoemission spectroscopy (ARPES) finds no clear evidence of any reconstruction [24–27], even for $La_{2-x}Sr_xCuO_4$ (LSCO) near $x = 1/8$ where signatures of reconstruction due to stripes are expected to be maximal [28,29]. A few recent studies report antinodal (AN) particle-hole symmetry breaking in the pseudogap phase of $Pb_{0.55}Bi_{1.55}Sr_{1.6}La_{0.4}CuO_{6+\delta}$ (Bi2201) [8,30], confirming the presence of competing order, but the underlying low-temperature dispersion of the electronic quasiparticles in the nodal region remains remarkably similar to that of a *d*-wave superconductor. This is still true even in the insulating spin-glass regime at doping levels so low that superconductivity is not yet present [26]. Here, we show that the absence of Fermi surface reconstruction can be attributed to strong spatial inhomogeneity of the competing phases that has been observed by numerous local probes [15–17,19–23]. This result contradicts conventional wisdom that disorder broadens spectral features but does not change the spectrum qualitatively.

Motivated by the widespread observation of slow short-range antiferromagnetic (AF) fluctuations in underdoped cuprates, we focus on the particular case of competition between AF and *d*-wave superconducting (dSC) order. Models with a single order parameter have been widely used to study the effect of superconducting phase [31–35], AF [36], or stripe [37] fluctuations on the quasiparticle spectrum with focus on the origin of the so-called Fermi arcs [38–50]. However, limited work has focussed on the complex problem of spatially heterogeneous competing order [51–53]. Because of the competition, thermal fluctuations of the AF and dSC fields, generated here by Monte Carlo (MC) simulations, produce a highly inhomogeneous state. Our main result is that the ARPES spectrum of this inhomogeneous state is qualitatively different from the case where AF and dSC order coexist homogeneously. We argue that this point is essential for a correct understanding of the ARPES spectra.

Our main results are illustrated in Fig. 1, where spectra are shown for pure dSC and competing dSC and AF (dSC + AF) order. Figures 1(a)–1(d)show snapshots, taken from the MC simulation, of the dSC amplitude $|\Delta_d(\mathbf{r}_i)|$ [Figs. 1(b) and 1(d)] and of the local AF moment $m_Q(\mathbf{r}_i)$ [Figs. 1(a) and 1(c)]. Figures 1(f) and 1(g) show the spectral function $A(\mathbf{k}, \omega)$ at k points taken along the nodal and AN lines shown in Fig. 1(e). These spectral functions arise from sampling configurations similar to those in Figs. 1(a) and 1(d). For comparison, in Fig. 1(h) we show spectra for the simplified case when dSC and AF order coexist homogeneously. In this case, we use the root-mean-square values of the AF and dSC order parameters from Fig. 1(g).

The similarity between the nodal spectra for the pure dSC and dSC + AF cases is remarkable, especially compared to the uniform dSC + AF case. In the uniform case [Fig. 1(h)], the nodal cut exhibits the well-known band backfolding that results in closed Fermi surface pockets around the AF Brillouin zone boundary. The backfolding is due to the AF band gap above the Fermi energy. It is striking that this band gap is completely absent in Fig. 1(g); instead, the dispersion is almost indistinguishable from that of the pure dSC, despite the sizable magnetic moment

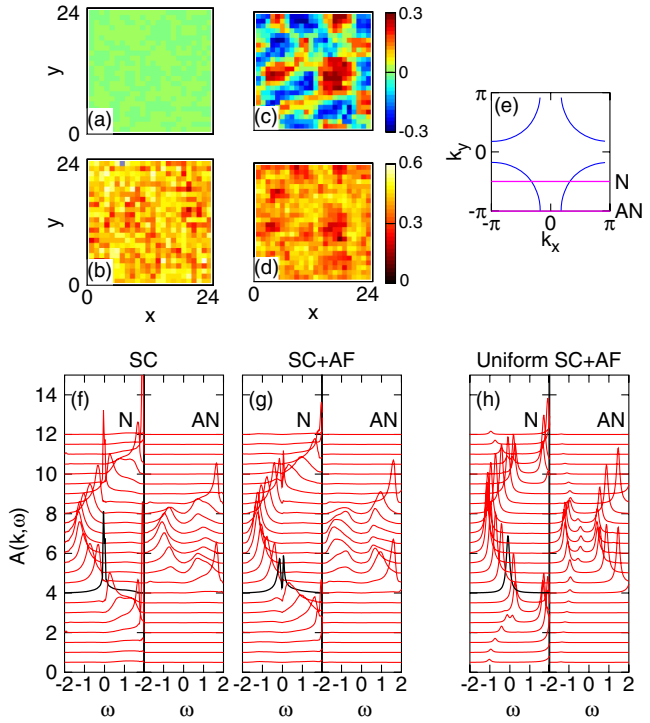

FIG. 1 (color online). (a)–(d) Snapshots from MC simulations for (a),(b) dSC and (c),(d) competing dSC and AF order at $T/T_c = 0.3$. (a),(c) $m_Q(\mathbf{r}_i)$ and (b),(d) $|\Delta_d(\mathbf{r}_i)|$ are shown. (f)–(h) MC-averaged spectral function along nodal (N) and antinodal (AN) cuts shown in (e) for (f) dSC, (g) dSC + AF, and (h) homogeneously coexisting dSC + AF. Linewidths are due to thermal fluctuations, except in (h) where a Lorentzian broadening of 0.1 was applied. The filling is $n \approx 0.88$, with $V = -1.0$ and (a),(b) $U = 0$ and (c),(d) $U = 3.5$. The Fermi energy is $\varepsilon_F = 0$. In (h) $\Delta_d = 0.35$ and $Um_Q = 3.5 \times 0.2$ based on average values in (g).

on nearly all sites [Fig. 1(c)]. The only signature of the competing magnetism is the narrow nodal gap at the Fermi energy, similar to what has been recently found in ARPES studies of underdoped LSCO [54]. In our model, the nodal gap appears only close to the superconductor-insulator transition; at smaller values of U, the nodal dispersion remains indistinguishable from the pure dSC case.

In contrast to the nodal spectrum, the AN spectrum for the uniform and inhomogeneous dSC + AF cases are qualitatively similar: the single quasiparticle peak at $\omega < \varepsilon_F$ in the pure dSC case is split by AF correlations into a pair of peaks, one of which is upward-dispersing and the other of which is downward-dispersing. While the splitting is obvious in Fig. 1(h), the peaks are not easily resolved in Fig. 1(g) because thermal broadening causes the lower intensity peak to appear as a shoulder.

The results shown in Fig. 1(g) are qualitatively similar to what has been reported at low T for ARPES experiments on Bi2201 [8,30]; namely, there is a band splitting at the antinode but no sign of Fermi surface reconstruction near the node. We emphasize that, while it is possible to model the AN spectrum with a uniform "finite-q" spin or charge density wave, as in Ref. [30], it is much more difficult to model the spectrum along the entire Fermi surface that way. Indeed, Norman *et al.* [48] argued against finite-q models of the pseudogap for this reason. Figure 1(g) shows that *fluctuating* finite-q order is consistent with ARPES experiments.

Figure 1 is based on MC simulations of an $L \times L$ lattice of electrons coupled to thermally fluctuating classical AF and dSC fields. The partition function is

$$Z = \int D[hdd^*] \exp[-\beta\Omega(h, d)], \tag{1}$$

where $\Omega(h, d) = -T \ln[\mathrm{Tr} \exp(-\beta\hat{H})]$, Tr... is a trace over electronic degrees of freedom, $\int D[hdd^*]\ldots$ is a $5L^2$-dimensional integral over the fields, and

$$\hat{H} = \sum_{ij\sigma} t_{ij} c^\dagger_{i\sigma} c_{j\sigma} - \sum_{i\sigma} \sigma h_i \hat{n}_{i\sigma} + \sum_i \frac{h_i^2}{U} + \sum_{ij} \left[d_{ij} c^\dagger_{i\uparrow} c^\dagger_{j\downarrow} + d^*_{ij} c_{j\downarrow} c_{i\uparrow} - \frac{|d_{ij}|^2}{V} \right]. \tag{2}$$

The real field h_i couples to the magnetization at site i, while the complex field d_{ij} couples to Cooper pairs along nearest-neighbor bonds between sites (i, j), and the integral over these fields in Eq. (1) is performed using a metropolis algorithm (see the Supplemental Material [55]). In Eq. (2), t_{ij} are the hopping matrix elements between nearest ($t_{ij} = -t = -1$; t is the unit of energy) and next-nearest ($t_{ij} = t' = 0.4$) neighbors. To reduce the number of integration variables, we impose the singlet constraint $d_{ij} = d_{ji}$. U and V control the size of the AF and dSC fields respectively; at $T = 0$, the saddle point approximation is exact and gives $h_i = Um(\mathbf{r}_i)$, where $m(\mathbf{r}_i) = \langle \hat{n}_{i\uparrow} - \hat{n}_{i\downarrow} \rangle / 2$, and $d_{ij} = V\langle c_{j\downarrow} c_{i\uparrow} \rangle$. The dSC order parameter is $\Delta_d(\mathbf{r}_i) = \sum_j (-1)^{y_i - y_j} \langle c_{j\downarrow} c_{i\uparrow} \rangle$, where j is summed over nearest neighbors of i, and the AF moment is $m_Q(\mathbf{r}_i) = (-1)^{x_i + y_i} m(\mathbf{r}_i)$. The dSC transition occurs at the temperature T_c where the pair correlation $\overline{\Delta_d(\mathbf{r}_i)\Delta^*_d(\mathbf{r}_i + \mathbf{R})} = 0$, with $\mathbf{R} = \frac{1}{2}(L, L)$. We fix $V = -1.0$, which sets an important energy scale: magnetic correlations become dominant at low T when $U|m(\mathbf{r}_i)| \gtrsim |V\Delta(\mathbf{r}_i)|$; here, this happens near $U = 3.5$.

Typical m_Q and Δ_d configurations sampled by the MC simulations shown in Fig. 2 illustrate how the model evolves with U. For $U = 3.3$ [Fig. 2(a)], there are large regions where $m_Q(\mathbf{r}_i)$ is negligible, and small pockets of short-lived AF order. Figure 2(b) shows a clear spatial anticorrelation between $\Delta_d(\mathbf{r}_i)$ and $m_Q(\mathbf{r}_i)$. In Fig. 2(c), we have plotted the local density of states (LDOS) at ε_F, calculated for the particular configurations shown in Figs. 2(a) and 2(b). The LDOS is reduced inside the AF pockets, and is largest in regions where the AF moments are smallest. Finally, in Fig. 2(d), we show the MC-averaged

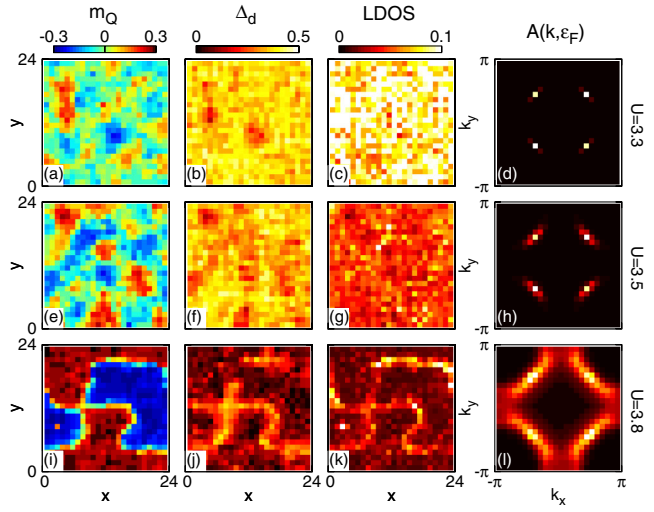

FIG. 2 (color online). Results of MC simulations at $T = 0.02$ for three different U values. Results are for (a)–(d) $U = 3.3$, (e)–(h) $U = 3.5$, and (i)–(l) $U = 3.8$. First and second columns contain MC snapshots of $m_Q(\mathbf{r}_i)$ and $|\Delta_d(\mathbf{r}_i)|$ respectively; the third column contains the LDOS at ε_F corresponding to the configuration in the first two columns. The final column shows the MC-averaged spectral function $A(\mathbf{k}, \varepsilon_F)$.

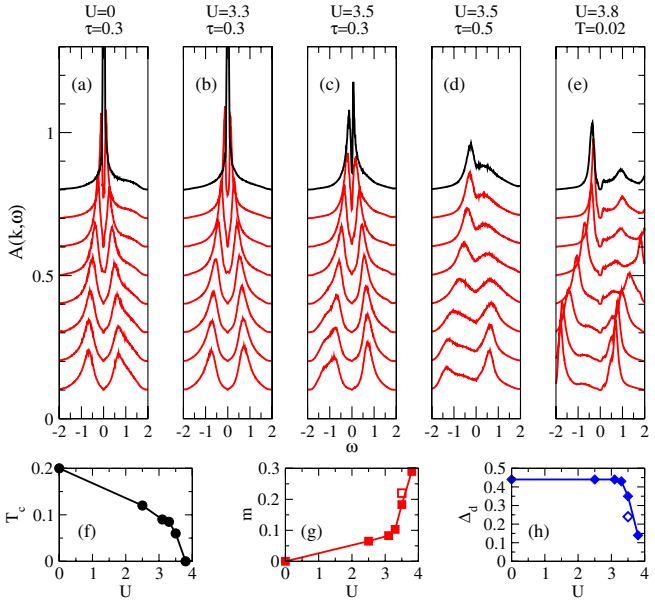

FIG. 3 (color online). Spectral function at k points along the Fermi surface (offset for clarity) between the nodal point (top curve; black) and the AN point (bottom curve). (a)–(e) correspond to different U or reduced temperature τ, and are arranged in order of increasing average magnetic moment. (f) T_c vs U and root-mean-square (g) m and (h) Δ_d at $\tau = 0.3$ (solid symbols) and $\tau = 0.5$ (open symbols).

spectral function at ε_F. It is apparent that the nodal quasiparticles are largely unaffected by the fluctuations, so that the low energy spectral weight is concentrated at the four nodal points.

The AF fluctuations are larger when $U = 3.5$ and Δ_d is suppressed in a significant fraction of the sample [Figs. 2(e) and 2(f)], although the maximum value of Δ_d is about the same as for $U = 3.3$. Typical AF domain sizes are 4–8 lattice constants, which is broadly consistent with tunneling experiments in underdoped cuprates [56]. The tendency for the low energy LDOS to be concentrated along AF domain walls is more pronounced in Fig. 2(g) than in Fig. 2(c) and becomes fully evident when $U = 3.8$ [Fig. 2(k)] where there is phase separation. In this case, mobile holes lie almost entirely at the boundaries between AF domains; there is some residual pairing of the holes [Fig. 2(j)], but there is no long-range phase coherence and the system is nonsuperconducting.

The spectral function for $U = 3.8$ [Fig. 2(l)] reveals surprisingly little of the complex real-space structure that emerges as U increases. The main change is that the nodal points in Fig. 2(d) evolve into "Fermi arcs" with increasing U. It is remarkable that for $U = 3.8$ one recovers the underlying "bare" Fermi surface purely from states along the spaghetti-like domain walls. This is reminiscent of the low-energy spectral features studied for disordered stripes [57,58], which, however, assumed perfect order along one spatial direction leading to a characteristic Fermi surface reconstruction.

Next, we show in Fig. 3 the progressive evolution of $A(\mathbf{k}, \omega)$ as the magnetic fluctuations are increased. The spectra are taken at momenta along the Fermi surface between the nodal and the AN points. To obtain good momentum resolution, we calculated the spectrum at k points that are interpolated, by introducing a complex boundary condition, between the L^2 k points of the original simulation. In Figs. 3(a)–3(c), $A(\mathbf{k}, \omega)$ is shown for increasing U at fixed reduced temperature $\tau \equiv T/T_c = 0.3$, and the root-mean-square values of Δ_d and m at this τ are plotted in Figs. 3(g) and 3(h). In Fig. 3(d), $\tau = 0.5$, which increases m and lowers Δ_d, as shown by the open symbols in Figs. 3(g) and 3(h). Finally, in Fig. 3(e), spectra are shown for the phase-separated system at low T.

As we found in Fig. 1, the $U = 0$ and $U = 3.3$ spectra are essentially indistinguishable, even though T_c is reduced by a factor of two by AF fluctuations in the latter case [Fig. 3(f)]. Small differences from the d-wave spectrum only emerge when $U = 3.5$ [Fig. 3(c)], by which point T_c is one third of its value at $U = 0$. When $U = 3.5$, a small gap appears at the node and the AN peak below ε_F splits into two. These features are more pronounced in Fig. 3(d), where the AF fluctuations are larger. Finally, there is a reorganization of the electronic structure into lower and upper magnetic bands when $U = 3.8$ [Fig. 3(e)]. It is the small residual spectral weight near ε_F, coming from the AF domain walls, which generates the Fermi surface in Fig. 2(l).

As mentioned above, a recent comprehensive ARPES study of LSCO has discovered that the excitation spectrum

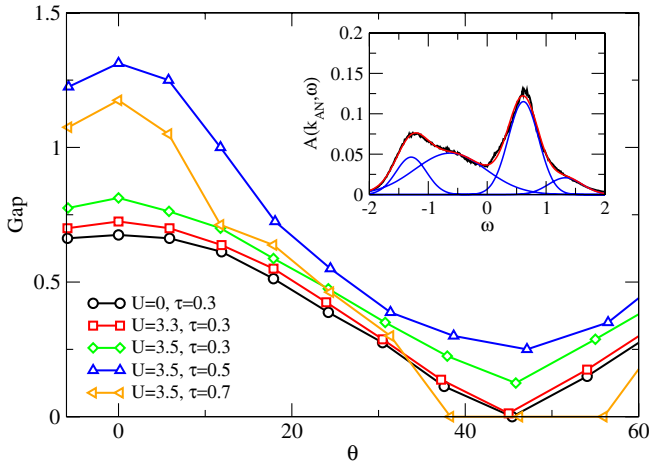

FIG. 4 (color online). Spectral gap along the Fermi surface for different U and τ. The angle θ is measured along the Fermi surface, with $\theta = 0°$ the antinode and $\theta = 45°$ the node. Inset: Gaussian decomposition of the antinodal spectrum for $U = 3.5$, $\tau = 0.5$.

is gapped along the entire underlying Fermi surface, and hence displays a nodal gap, in the highly underdoped regime [54]. At doping levels where the nodal gap is observed, a spin glass is known to coexist with superconductivity [23], and in Fig. 4 we show that AF fluctuations can indeed generate a nodal gap.

Figure 4 shows how the gap along the Fermi surface depends on both the magnitude and the correlation length of the AF fluctuations. To be consistent with experiments, we define the gap at a point $\mathbf{k}$ on the Fermi surface as the energy of the peak in $A(\mathbf{k}, \omega)$ with the smallest binding energy, for $\omega < \varepsilon_F$. When $U \leq 3.3$, the gap along the Fermi surface has a dSC-like structure, and is characterized by a single energy scale. When AF correlations are stronger (see, e.g., the $U = 3.5$, $\tau = 0.3$ curve) the AN gap remains set by the dSC scale, and a second energy scale emerges in the form of a small gap at the node, similar to what was found by Razzoli *et al.* [54]. In Fig. 4, the nodal gap grows with the AF magnitude, but vanishes at high temperature when the AF correlation length is short and line broadening wipes it out. A third energy scale emerges at the antinode when AF correlations are strong ($U = 3.5$ and $\tau \geq 0.5$). In this case, a large gap, with an energy scale distinct from that near the node, develops. Similar crossovers between a superconducting nodal gap and nonsuperconducting AN gap have been widely seen in ARPES experiments on many underdoped cuprates [1,3,5,6,8,10]; that this is not reported in LSCO suggests that AF correlations are not strong enough for a clear AN feature to develop.

We have found that, even when they cannot be resolved by eye, two energy scales are always present in the AN spectrum when U is large enough that sizable local moments form (Fig. 4 inset). The inner peak has a d-wave k-space structure, while the outer peak is tied to the AF fluctuations, although it is not simply related to the magnetic energy scale ($Um \sim 0.7$ in the inset). To confirm AF correlations as the source of the nodal gap in LSCO, our calculations suggest to look for a second energy scale, particularly in the AN spectrum. This would distinguish spin glass physics from models (such as $d + id$ pairing [54]) in which the gaps are added in quadrature.

In conclusion, we have shown that the overall spectrum measured by ARPES experiments is consistent with simple models of competing order if one accounts for the highly inhomogeneous nature of the competing phases. This work reconciles the simple Fermi surface structure measured by ARPES with the highly inhomogeneous electronic structure measured by local probes.

W. A. A. and J. D. B. acknowledge support by the Natural Sciences and Engineering Research Council (NSERC) of Canada. This work was made possible by the facilities of the Shared Hierarchical Academic Research Computing Network and Compute/Calcul Canada.

*billatkinson@trentu.ca

[1] K. Tanaka, W. S. Lee, D. H. Lu, A. Fujimori, T. Fujii, Risdiana, I. Terasaki, D. J. Scalapino, T. P. Devereaux, Z. Hussain, and Z.-X. Shen, Science **314**, 1910 (2006).
[2] M. Le Tacon, A. Sacuto, A. Georges, G. Kotliar, Y. Gallais, D. Colson, and A. Forget, Nat. Phys. **2**, 537 (2006).
[3] W. S. Lee, I. M. Vishik, K. Tanaka, D. H. Lu, T. Sasagawa, N. Nagaosa, T. P. Devereaux, Z. Hussain, and Z. X. Shen, Nature (London) **450**, 81 (2007).
[4] N. Doiron-Leyraud, C. Proust, D. LeBoeuf, J. Levallois, J.-B. Bonnemaison, R. Liang, D. A. Bonn, W. N. Hardy, and L. Taillefer, Nature (London) **447**, 565 (2007).
[5] J.-H. Ma, Z.-H. Pan, F. C. Niestemski, M. Neupane, Y.-M. Xu, P. Richard, K. Nakayama, T. Sato, T. Takahashi, H.-Q. Luo, L. Fang, H.-H. Wen, Z. Wang, H. Ding, and V. Madhavan, Phys. Rev. Lett. **101**, 207002 (2008).
[6] T. Kondo, R. Khasanov, T. Takeuchi, J. Schmalian, and A. Kaminski, Nature (London) **457**, 296 (2009).
[7] R. Daou, J. Chang, D. LeBoeuf, O. Cyr-Choinière, F. Laliberté, N. Doiron-Leyraud, B. J. Ramshaw, R. Liang, D. A. Bonn, W. N. Hardy, and Louis Taillefer, Nature (London) **463**, 519 (2010).
[8] R.-H. He, M. Hashimoto, H. Karapetyan, J. D. Koralek, J. P. Hinton, J. P. Testaud, V. Nathan, Y. Yoshida, H. Yao, K. Tanaka *et al.*, Science **331**, 1579 (2011).
[9] T. Wu, H. Mayaffre, S. Krämer, M. Horvatic, C. Berthier, W. N. Hardy, R. Liang, D. A. Bonn, and M.-H. Julien, Nature (London) **477**, 191 (2011).
[10] S.-I. Ideta, T. Yoshida, A. Fujimori, H. Anzai, T. Fujita, A. Ino, M. Arita, H. Namatame, M. Taniguchi, Z.-X. Shen, K. Takashima, K. Kojima, and S.-i. Uchida, Phys. Rev. B **85**, 104515 (2012).
[11] S. A. Kivelson, I. P. Bindloss, E. Fradkin, V. Oganesyan, J. M. Tranquada, A. Kapitulnik, and C. Howald, Rev. Mod. Phys. **75**, 1201 (2003).

[12] V. Hinkov, D. Haug, B. Fauqué, P. Bourges, Y. Sidis, A. Ivanov, C. Bernhard, C. T. Lin, and B. Keimer, Science **319**, 597 (2008).

[13] D. Haug, V. Hinkov, Y. Sidis, P. Bourges, N. B. Christensen, A. Ivanov, T. Keller, C. T. Lin, and B. Keimer, New J. Phys. **12**, 105006 (2010).

[14] G. Ghiringhelli, M. Le Tacon, M. Minola, S. Blanco-Canosa, C. Mazzoli, N. B. Brookes, G. M. De Luca, A. Frano, D. G. Hawthorn, F. He *et al.*, Science **337**, 821 (2012).

[15] C. Howald, H. Eisaki, N. Kaneko, M. Greven, and A. Kapitulnik, Phys. Rev. B **67**, 014533 (2003).

[16] M. Vershinin, S. Misra, S. Ono, Y. Abe, Y. Ando, and A. Yazdani, Science **303**, 1995 (2004).

[17] Y. Kohsaka, C. Taylor, K. Fujita, A. Schmidt, C. Lupien, T. Hanaguri, M. Azuma, M. Takano, H. Eisaki, H. Takagi, S. Uchida, and J. C. Davis, Science **315**, 1380 (2007).

[18] B. Fauqué, Y. Sidis, V. Hinkov, S. Pailhès, C. T. Lin, X. Chaud, and P. Bourges, Phys. Rev. Lett. **96**, 197001 (2006).

[19] C. Niedermayer, C. Bernhard, T. Blasius, A. Golnik, A. Moodenbaugh, and J. I. Budnick, Phys. Rev. Lett. **80**, 3843 (1998).

[20] T. Suzuki, T. Goto, K. Chiba, T. Shinoda, T. Fukase, H. Kimura, K. Yamada, M. Ohashi, and Y. Yamaguchi, Phys. Rev. B **57**, R3229 (1998).

[21] M.-H. Julien, F. Borsa, P. Carretta, M. Horvatić, C. Berthier, and C. T. Lin, Phys. Rev. Lett. **83**, 604 (1999).

[22] A. T. Savici, Y. Fudamoto, I. M. Gat, T. Ito, M. I. Larkin, Y. J. Uemura, G. M. Luke, K. M. Kojima, Y. S. Lee, M. A. Kastner, R. Birgeneau, and K. Yamada, Phys. Rev. B **66**, 014524 (2002).

[23] C. Panagopoulos, J. L. Tallon, B. D. Rainford, J. R. Cooper, C. A. Scott, and T. Xiang, Solid State Commun. **126**, 47 (2003).

[24] A. Damascelli, Z. Hussain, and Z.-X. Shen, Rev. Mod. Phys. **75**, 473 (2003).

[25] A. Kanigel, U. Chatterjee, M. Randeria, M. R. Norman, S. Souma, M. Shi, Z. Z. Li, H. Raffy, and J. C. Campuzano, Phys. Rev. Lett. **99**, 157001 (2007).

[26] U. Chatterjee, M. Shi, D. Ai, J. Zhao, A. Kanigel, S. Rosenkranz, H. Raffy, Z. Z. Li, K. Kadowaki, D. G. Hinks, Z. J. Xu, J. S. Wen, G. Gu, C. T. Lin, H. Claus, M. R. Norman, M. Randeria, and J. C. Campuzano, Nat. Phys. **6**, 99 (2009).

[27] H.-B. Yang, J. D. Rameau, Z.-H. Pan, G. D. Gu, P. D. Johnson, H. Claus, D. G. Hinks, and T. E. Kidd, Phys. Rev. Lett. **107**, 047003 (2011).

[28] J. Chang, Y. Sassa, S. Guerrero, M. Månsson, M. Shi, S. Pailhés, A. Bendounan, R. Mottl, T. Claesson, O. Tjernberg, L Patthey, M Ido, M Oda, N Momono, C Mudry, and J Mesot, New J. Phys. **10**, 103016 (2008).

[29] R.-H. He, X. J. Zhou, M. Hashimoto, T. Yoshida, K. Tanaka, S.-K. Mo, T. Sasagawa, N. Mannella, W. Meevasana, H. Yao *et al.*, New J. Phys. **13**, 013031 (2011).

[30] M. Hashimoto, R.-H. He, K. Tanaka, J.-P. Testaud, W. Meevasana, R. G. Moore, D. Lu, H. Yao, Y. Yoshida, H. Eisaki, T. P. Devereaux, Z. Hussain, and Z.-X. Shen, Nat. Phys. **6**, 414 (2010).

[31] T. Eckl, D. J. Scalapino, E. Arrigoni, and W. Hanke, Phys. Rev. B **66**, 140510 (2002).

[32] M. Mayr, G. Alvarez, C. Şen, and E. Dagotto, Phys. Rev. Lett. **94**, 217001 (2005).

[33] D. Valdez-Balderas and D. Stroud, Phys. Rev. B **74**, 174506 (2006).

[34] S. Banerjee, T. V. Ramakrishnan, and C. Dasgupta, Phys. Rev. B **84**, 144525 (2011).

[35] Y.-W. Zhong, T. Li, and Q. Han, Phys. Rev. B **84**, 024522 (2011).

[36] N. Harrison, R. McDonald, and J. Singleton, Phys. Rev. Lett. **99**, 206406 (2007).

[37] M. Vojta, Phys. Rev. B **78**, 144508 (2008).

[38] S. Chakravarty, C. Nayak, and S. Tewari, Phys. Rev. B **68**, 100504 (2003).

[39] C. Li, S. Zhou, and Z. Wang, Phys. Rev. B **73**, 060501 (2006).

[40] K.-Y. Yang, T. M. Rice, and F.-C. Zhang, Phys. Rev. B **73**, 174501 (2006).

[41] T. D. Stanescu and G. Kotliar, Phys. Rev. B **74**, 125110 (2006).

[42] C. M. Varma and L. Zhu, Phys. Rev. Lett. **98**, 177004 (2007).

[43] A. Paramekanti and E. Zhao, Phys. Rev. B **75**, 140507 (2007).

[44] A. M. Tsvelik and A. V. Chubukov, Phys. Rev. Lett. **98**, 237001 (2007).

[45] R. Sensarma, M. Randeria, and N. Trivedi, Phys. Rev. Lett. **98**, 027004 (2007).

[46] R. K. Kaul, A. Kolezhuk, M. Levin, S. Sachdev, and T. Senthil, Phys. Rev. B **75**, 235122 (2007).

[47] B. Valenzuela and E. Bascones, Phys. Rev. Lett. **98**, 227002 (2007).

[48] M. R. Norman, A. Kanigel, M. Randeria, U. Chatterjee, and J. C. Campuzano, Phys. Rev. B **76**, 174501 (2007).

[49] M. Granath and B. M. Andersen, Phys. Rev. B **81**, 024501 (2010).

[50] Q. Han, T. Li, and Z. D. Wang, Phys. Rev. B **82**, 052503 (2010).

[51] G. Alvarez, M. Mayr, A. Moreo, and E. Dagotto, Phys. Rev. B **71**, 014514 (2005).

[52] G. Alvarez and E. Dagotto, Phys. Rev. Lett. **101**, 177001 (2008).

[53] M. Vojta, T. Vojta, and R. K. Kaul, Phys. Rev. Lett. **97**, 097001 (2006).

[54] E. Razzoli, G. Drachucki, A. Keren, M. Radovic, N. C. Plumb, J. Chang, J. Mesot, and M. Shi, arXiv:1207.3486v1.

[55] See Supplemental Material at http://link.aps.org/supplemental/10.1103/PhysRevLett.109.267004 for a description of the Monte Carlo algorithm.

[56] A. R. Schmidt, K. Fujita, E.-A. Kim, M. J. Lawler, H. Eisaki, S. Uchida, D.-H. Lee, and J. C. Davis, New J. Phys. **13**, 065014 (2011).

[57] M. I. Salkola, V. J. Emery, and S. A. Kivelson, Phys. Rev. Lett. **77**, 155 (1996).

[58] M. Granath, V. Oganesyan, D. Orgad, and S. A. Kivelson, Phys. Rev. B **65**, 184501 (2002).